6-15-2012

LapG, Required for Modulating Biofilm Formation by Pseudomonas fluorescens Pf0-1, Is a Calcium-Dependent Protease

Chelsea D. Boyd
Dartmouth College

Debashree Chatterjee
Cornell University

Holger Sondermann
Cornell University

George A. O'Toole
Dartmouth College

JB
Journals.ASM.org

LapG, Required for Modulating Biofilm Formation by *Pseudomonas fluorescens* Pf0-1, Is a Calcium-Dependent Protease

Chelsea D. Boyd,[a] Debashree Chatterjee,[b] Holger Sondermann,[b] and George A. O'Toole[a]

Department of Microbiology and Immunology, Geisel School of Medicine at Dartmouth, Hanover, New Hampshire, USA,[a] and Department of Molecular Medicine, College of Veterinary Medicine, Cornell University, Ithaca, New York, USA[b]

Biofilm formation by *Pseudomonas fluorescens* Pf0-1 requires the cell surface adhesin LapA. We previously reported that LapG, a periplasmic cysteine protease of *P. fluorescens*, cleaves the N terminus of LapA, thus releasing this adhesin from the cell surface and resulting in loss of the ability to make a biofilm. The activity of LapG is regulated by the inner membrane-localized cyclic-di-GMP receptor LapD via direct protein-protein interactions. Here we present chelation and metal add-back studies demonstrating that calcium availability regulates biofilm formation by *P. fluorescens* Pf0-1. The determination that LapG is a calcium-dependent protease, based on *in vivo* and *in vitro* studies, explains the basis of this calcium-dependent regulation. Based on the crystal structure of LapG of *Legionella pneumophila* in the accompanying report by Chatterjee and colleagues (D. Chatterjee et al., J. Bacteriol. 194:4415–4425, 2012), we show that the calcium-binding residues of LapG, D134 and E136, which are near the critical C135 active-site residue, are required for LapG activity of *P. fluorescens in vivo* and *in vitro*. Furthermore, we show that mutations in D134 and E136 result in LapG proteins no longer able to interact with LapD, indicating that calcium binding results in LapG adopting a conformation competent for interaction with the protein that regulates its activity. Finally, we show that citrate, an environmentally relevant calcium chelator, can impact LapG activity and thus biofilm formation, suggesting that a physiologically relevant chelator of calcium can impact biofilm formation by this organism.

Bacteria sense and respond to fluctuating environmental nutrients and signals to coordinate adaptive changes in metabolic pathways and physiological outputs. Integration of environmental cues affords bacteria the ability to make important decisions regarding how to respond to their constantly changing environments. When coming in contact with a surface, whether in natural, industrial, or clinical settings, bacteria must evaluate whether the surface and the local environment are favorable for attachment.

Initial colonization of a surface is the first step in biofilm formation. This transition from a planktonic to a sessile lifestyle is often in response to a variety of environmental cues, such as osmolarity, pH, carbon, iron availability, oxygen tension, and temperature (14, 15, 19, 32–35, 37, 40, 43). Colonization of a surface and the subsequent development of a biofilm involve an array of cellular factors and diverse molecular mechanisms. However, a unifying theme across bacterial species is that synthesis of the cellular signaling molecule bis-(3′-5′)-cyclic dimeric GMP (c-di-GMP), a central player in the signaling networks that control biofilm formation, coincides with the transition to a sessile lifestyle.

Pseudomonas fluorescens Pf0-1, a model organism for biofilm research, is a biological control agent that promotes plant growth by forming biofilms on plant roots (10). The environmental nutrient P_i has been shown to be an important signal regulating the switch between a planktonic and a sessile lifestyle in *P. fluorescens* (23, 24). Work by our group identified a large adhesive protein, LapA, required for the attachment of *P. fluorescens* (12). Subsequent studies have elucidated a c-di-GMP signaling system that regulates biofilm formation through posttranslational modification of LapA (26–28). In short, under conditions that do not favor biofilm formation, such as low P_i, the periplasmic cysteine protease LapG cleaves LapA from the cell surface, thus releasing the adhesin and preventing attachment (28). LapG activity is regulated by the inner membrane c-di-GMP effector protein LapD. LapD binds c-di-GMP and undergoes conformational changes (26, 27), and through an inside-out signaling mechanism that is dependent upon c-di-GMP, LapD binds LapG, preventing LapG-dependent cleavage of LapA from the cell surface. Thus, under conditions that favor biofilm formation, LapA remains at the cell surface, promoting biofilm formation (28).

While we have a detailed picture of the LapD-LapG c-di-GMP control circuit, from the environmental P_i input to the LapA output that regulates biofilm formation in *P. fluorescens* Pf0-1, much less is known about how *P. fluorescens* regulates biofilm formation in response to other environmental nutrients. Calcium (Ca^{2+}) regulates cellular function in bacteria and is involved in many different processes, such as adhesion, cell cycle and cell division, pathogenesis, motility, chemotaxis, and quorum sensing (6, 8, 13, 22, 30, 31, 41). Ca^{2+} has been shown to both inhibit and stimulate biofilm formation in bacterial species that also encode large adhesion proteins that mediate biofilm formation (2, 42).

In this study and in the accompanying report by Chatterjee and colleagues (3), we describe the analysis of the LapG protease. LapG belongs to the domain of unknown function 920 (DUF920) (or COG3672) family. Aside from previous studies by our group demonstrating that LapG is a cysteine protease that functions to cleave LapA from the cell surface (28), little is known regarding the function of LapG. Here we present genetic and biochemical studies demonstrating that the LapG protease of *P. fluorescens* Pf0-1 is a

Received 16 April 2012 **Accepted** 8 June 2012
Published ahead of print 15 June 2012
Address correspondence to George A. O'Toole, georgeo@dartmouth.edu.
Supplemental material for this article may be found at http://jb.asm.org/.

doi:10.1128/JB.00642-12

Ca^{2+}-dependent enzyme. These findings are supported and extended by the accompanying report by Chatterjee and colleagues, which presents the structure of the LapG homolog of *Legionella pneumophila* (3).

MATERIALS AND METHODS

Strains and media. The strains and plasmids used in this study are listed in Table S1 in the supplemental material. SMC 4798, described previously (23, 28, 29), is the wild-type (WT) *P. fluorescens* strain used in this study. *P. fluorescens* strain SMC 4798 carries three hemagglutinin (HA) epitope tags within a fully functional, chromosomally encoded LapA protein. *P. fluorescens* and *Escherichia coli* were routinely cultured with liquid LB medium in a test tube or on solidified LB with 1.5% agar and grown at 30°C or 37°C, respectively. Gentamicin was used at 30 μg/ml for *P. fluorescens* and at 10 μg/ml for *E. coli*. Tetracycline was used at 30 μg/ml on plates and at 15 μg/ml in liquid culture for *P. fluorescens*. Kanamycin was used at 30 μg/ml for *P. fluorescens*. Ampicillin (Amp) was used at 100 μg/ml for *E. coli*. Arabinose was used to induce expression from pMQ72 at 0.2% for complementation and overexpression experiments. Isopropyl-β-D-thiogalactopyranoside (IPTG) at 1 mM was used to induce expression from pET21. *P. fluorescens* was grown in K10T-1 medium for biofilm assays, LapA localization, protein expression, and coprecipitations. K10T-1 was previously described as a phosphate-rich medium (24).

Biofilm formation assays. Biofilm formation assays were performed exactly as previously described (29). EDTA (Fisher), EGTA (Sigma-Aldrich), calcium chloride ($CaCl_2$; Sigma-Aldrich), magnesium chloride ($MgCl_2$; Fisher), ferric chloride ($FeCl_3$; Sigma-Aldrich), cupric chloride ($CuCl_2$; Sigma-Aldrich), zinc chloride ($ZnCl_2$; Sigma-Aldrich), and manganese chloride ($MnCl_2$; Sigma-Aldrich) were added to biofilm assays at the beginning of the assay at a final concentration of 500 μM. Sodium citrate (Fisher) was added at the start of the biofilm assay at a final concentration of 0.4% (wt/vol). Staining, imaging, and quantification of attached biofilm biomass were also performed as previously described (23).

Constructs for clean deletion of Calx-β and complementation and overexpression of LapG variants. *Saccharomyces cerevisiae* strain InvSci (Invitrogen) was used to construct plasmids for clean deletion, complementation, and overexpression experiments through *in vivo* homologous recombination as previously described (39). All deletion mutants were constructed by the same basic strategy as previously described (29).

Complementation and overexpression studies utilized the pMQ72 plasmid as previously described (29). LapG-D134A and LapG-E136A site-directed mutations were made as previously described (29). Briefly, two fragments were amplified by PCR either from the LapG complementation plasmid template containing a six-histidine (6H) tag or from the LapG-HA LapD-6H complementation plasmid template (28) using a primer on the vector backbone and a primer divergent from and excluding the codon for either Asp or Glu in the calcium-binding site. Divergent primers included additional bases encoding Ala replacement codons, as well as sequence to facilitate yeast recombination. Yeast was transformed with pMQ72 and both PCR fragments, resulting in a plasmid identical to the parent, except for the point mutation at the calcium-binding residue. Sequencing confirmed the successful construction of each plasmid and chromosomal alteration.

LapA localization. For Western and dot blot assays of the LapA protein, we used strains with internal HA tags in the chromosomal *lapA* gene. Culturing conditions, preparation of clarified cell extracts, and analysis of samples for LapA localization were performed exactly as previously described (23, 28). Detection of cell surface LapA by dot blotting was also performed as previously described (27, 28). To test the effects of the addition of EGTA, EDTA, $CaCl_2$, or $MgCl_2$ on LapA localization, each compound was added at the beginning of the 6-h subculturing period to a final concentration of 500 μM.

Protein purification. The periplasmic, signal sequence-processed module of *P. fluorescens* LapG (residues 50 to 251) was cloned, expressed, and purified by standard molecular biology and chromatography techniques as described previously (26). Briefly, the gene was amplified by standard PCR and cloned into a pET21 expression plasmid (Novagen) producing a C-terminally 6H-tagged protein. LapG point mutants for biochemical studies were generated by using a QuikChange site-directed mutagenesis kit (Stratagene) and following the manufacturer's instructions. The WT and mutant proteins were expressed in T7 Express cells (New England BioLabs) and grown at 37°C in terrific broth medium supplemented with 100 μg/ml Amp. At an optical density at 600 nm of ~1, the temperature was reduced to 18°C and protein expression was induced by the addition of 1 mM IPTG. After 16 h of expression at 18°C, cells were harvested by centrifugation, resuspended in Ni-nitrilotriacetic acid (NTA) buffer A (25 mM Tris-HCl [pH 8.5], 500 mM NaCl, 20 mM imidazole), and flash frozen in liquid nitrogen. Following thawing and cell lysis by sonication, the cell debris was removed by centrifugation and the clear lysates were incubated with Ni-NTA resin (Qiagen) that was pre-equilibrated with Ni-NTA buffer A. After the lysates were allowed to flow through, the resins were washed with 20 column volumes of buffer A and proteins were eluted with 5 column volumes of Ni-NTA buffer B (25 mM Tris-HCl [pH 8.5], 500 mM NaCl, 300 mM imidazole). The eluted proteins were subjected to size exclusion chromatography on a Superdex 200 column (GE Healthcare) preequilibrated with gel filtration buffer (25 mM Tris [pH 8.5], 150 mM NaCl). The proteins were concentrated on Amicon filters with an appropriate molecular size cutoff, flash frozen in liquid nitrogen, and stored at −80°C. Protein purity was determined by SDS-PAGE and was estimated to be ~95%. Purification of N-Term-LapA-6H from *E. coli* was done by standard nickel affinity chromatography techniques as previously described (20).

LapG activity assays. Bacterial cultures were grown in the same manner, and clarified cell extracts were prepared as for LapA localization, as described previously (23, 28). LapG activity assays with mini-LapA and N-Term-LapA were performed as previously described (28). Assays incorporated 375 ng of LapG, D134A LapG, or E136A LapG. Activity assays were performed in the presence of 500 μM EGTA, $CaCl_2$, or $MgCl_2$ or 0.4% (wt/vol) sodium citrate, as indicated.

Coprecipitations. Proteins were precipitated from clarified cell extracts prepared in the same manner as described above for LapA localization (23, 28). Coimmunoprecipitation with nickel resin was preformed exactly as previously described (28).

Statistical analysis. Statistical analysis of the data presented utilized the Student *t* test, analysis of variance with Tukey's honest significant difference as a posttest, or linear models, as appropriate. Significance was set at the traditional 95% confidence interval.

RESULTS

EGTA chelation induces a hyperadherent biofilm phenotype. Calcium (Ca^{2+}) has been shown to both inhibit and stimulate biofilm formation in bacterial species that encode large adhesion proteins that mediate biofilm formation (2, 42). To test the requirement of Ca^{2+} for biofilm formation in *P. fluorescens*, we individually supplemented the biofilm medium K10T-1 with the chelating agent EDTA or EGTA. EDTA has a strong affinity for iron ions and a much weaker affinity for Ca^{2+} (4), while EGTA has a strong affinity for Ca^{2+} and a much weaker affinity for magnesium ions (Mg^{2+}) (44).

WT *P. fluorescens* biofilm biomass in the static microtiter dish biofilm assay was not statistically significantly different ($P > 0.05$) in the presence of EDTA, but the biofilm formed by the WT supplemented with EGTA was significantly increased ($P < 0.05$) and more than twice that of the WT grown in K10T-1 (Fig. 1A). Chelation by EGTA impacts the initial stage of biofilm formation, as an accumulation of biofilm biomass begins at the 2-h time point and continues through the endpoint of the assay at 6 h (see Fig. S1 in the supplemental material). Growth of *P. fluorescens* was unaffected by the addition of these chelating agents at the concentra-

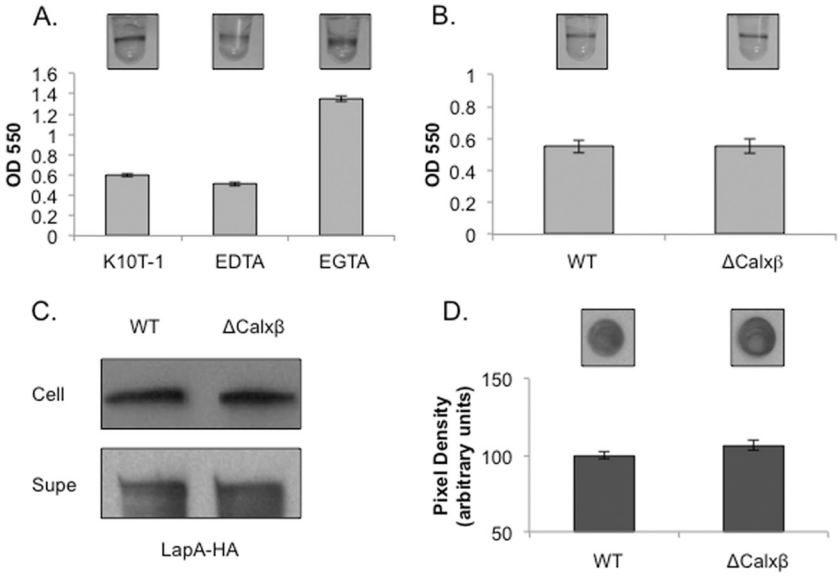

FIG 1 Chelation by EGTA stimulates biofilm formation. (A) The chelator EGTA stimulates biofilm formation. Shown is the biofilm formation of WT *P. fluorescens* Pf0-1 grown in K10T-1 medium alone or supplemented with EDTA or EGTA at 500 μM. Assay mixtures were incubated for 6 h at 30°C before being stained with crystal violet and quantified. The *y* axis shows the optical density at 550 nm (OD 550) of the extracted crystal violet used to determine the bacterial biofilm biomass. (B) Deletion of the Calxβ domain has no impact on biofilm formation. Shown is a biofilm formation assay of the WT and a strain with a LapA variant with the Calxβ domain deleted. The biofilm assay was performed as outlined for panel A. (C) Levels and localization of LapA in whole-cell and supernatant fractions. Shown is a Western blot assay of the levels of WT LapA and the LapA ΔCalxβ variant in the whole-cell (Cell) and supernatant (Supe) fractions. Here and in all subsequent figures, LapA was detected via an engineered HA tag as described in Materials and Methods. (D) Cell surface levels of LapA. Shown are a representative dot blot assay (top) and quantification of the pixel density of six to eight replicates (bottom) to assess the level of cell surface LapA of the WT or the strain expressing the LapA ΔCalxβ variant.

tions used here (data not shown). Given the high affinity of EGTA for Ca^{2+}, our findings are consistent with a role for Ca^{2+} in biofilm formation. These results suggest that decreasing the Ca^{2+} concentration stimulates biofilm formation and induces a hyperadherent biofilm phenotype.

The Calx-β domain of LapA is not required for calcium-dependent changes in biofilm formation. LapA contains a Calx-β Ca^{2+}-binding domain, indicating that LapA may directly bind Ca^{2+}, thus possibly explaining the increased biofilm formation seen after the addition of EGTA. The Calx-β domain was initially identified in Na^{+}-Ca^{2+} exchangers of eukaryotic systems, which expel Ca^{2+} from the cytoplasm (1, 21, 38). Given the presence of the Calx-β domain, we hypothesized that this domain may be required for Ca^{2+}-mediated effects on biofilm formation.

To assess the requirement of the Calx-β domain for biofilm formation, we deleted the domain from LapA (this domain spans amino acids T4049 to 4094D). Deletion of the domain did not result in a change in biofilm biomass compared to that of the WT (Fig. 1B). Consistent with no apparent impact on biofilm formation, we also observed no difference in the levels of LapA in the cellular, supernatant, or cell surface fractions in the WT compared to those in the strain with the LapA variant with the Calx-β domain deleted (Fig. 1C and D). A control study demonstrating the specificity of LapA detection in these fractions is presented in Fig. S2 in the supplemental material. Furthermore, supplementation of the K10T-1 medium with $CaCl_2$, EDTA, or EGTA did not affect the biofilm phenotype of the Calx-β mutant compared to that of the WT (see Fig. S3A in the supplemental material) or alter the localization of LapA in the Calx-β mutant (see Fig. S3B and C in the supplemental material). Together, these data suggest that the Calx-β domain of LapA is not required for chelator- or Ca^{2+}-mediated effects on biofilm formation.

Calcium rescues the chelation-induced hyperadherent biofilm phenotype. Given that EGTA has an affinity for both Ca^{2+} and Mg^{2+}, we hypothesized that addition of $CaCl_2$ or magnesium chloride ($MgCl_2$) to the biofilm assay might reverse the effects of the EGTA-induced hyperadherent biofilm phenotype. The WT hyperadherent biofilm phenotype was reversed in the presence of EGTA and 500 μM $CaCl_2$ compared to that in the presence of EGTA alone (Fig. 2A) but not when 500 μM $MgCl_2$ was added to the EGTA-treated WT strain (Fig. 2B; see Fig. S4 in the supplemental material).

K10T-1 contains 610 μM $MgSO_4$ to support bacterial growth. To chelate the Mg^{2+} contained in the K10T-1 medium, chelation experiments were also performed with 1 mM EGTA. Addition of 1 mM or 2.5 mM $MgCl_2$ did not reverse the WT hyperadherent biofilm phenotype (see Fig. S4A in the supplemental material), suggesting that changes in the Mg^{2+} concentration are not responsible for the alteration in biofilm formation. Other metal ions were tested for the ability to reduce the EGTA-induced hyperadherent biofilm. Ferric chloride, cupric chloride, zinc chloride, and manganese chloride, all at 500 μM, did not reverse the effects of the EGTA-induced hyperadherent biofilm (data not shown). Growth of *P. fluorescens* was unaffected by the addition of metal ions at the concentrations used here (data not shown). We also supplemented the medium (in the absence of EGTA) with $CaCl_2$ or $MgCl_2$ to assess the effects on biofilm formation of the WT. Neither Ca^{2+} nor Mg^{2+} significantly affected biofilm biomass (Fig. 2A and B). Together, these data suggest that EGTA chelation causes a hyperadherent biofilm phenotype due to the loss of Ca^{2+}.

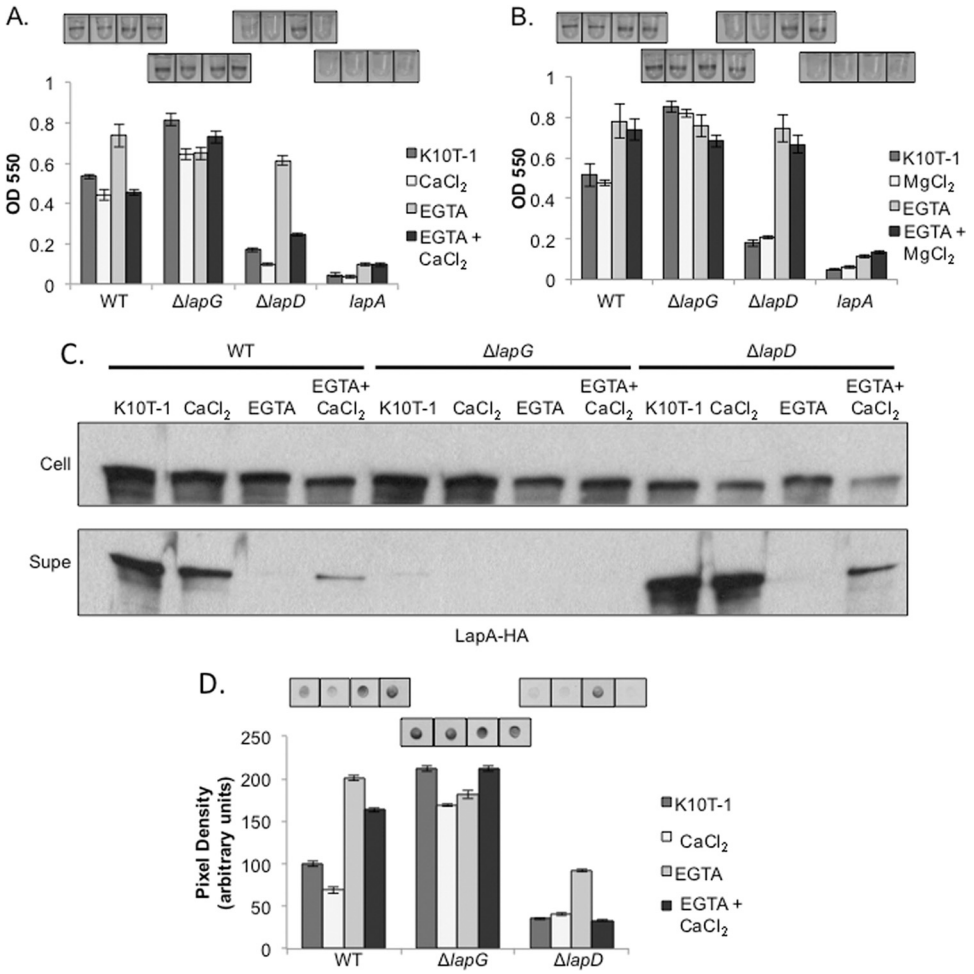

FIG 2 Calcium chelation stimulates biofilm formation. (A) Calcium depletion by EGTA stimulates biofilm formation. Shown are biofilm assays of the WT and the Δ*lapG*, Δ*lapD*, and *lapA* mutants grown in K10T-1 medium or in this medium supplemented with $CaCl_2$ (500 μM), EGTA (500 μM), or both. The *y* axis shows the optical density at 550 nm (OD 550) of the extracted crystal violet used to determine the bacterial biofilm biomass. (B) Magnesium does not reverse EGTA-stimulated biofilm formation. Assays were performed as described for panel A but with $MgCl_2$ (500 μM) in place of $CaCl_2$. (C) Levels and localization of LapA in whole-cell and supernatant fractions. Shown is a Western blot assay of the levels of LapA in the whole-cell (Cell) and supernatant (Supe) fractions of the strains indicated under the treatment conditions indicated. (D) Cell surface levels of LapA. Shown is a representative dot blot assay (top) and quantification of the pixel density of six to eight replicates (bottom) to assess the levels of cell surface LapA fractions of the strains indicated under the treatment conditions indicated.

We also examined the impacts of Ca^{2+} alone, EGTA alone, and EGTA plus Ca^{2+} on LapA levels and localization in the WT. These treatments did not alter the cellular level of LapA (Fig. 2C), but consistent with the phenotypes shown in Fig. 2A, treatment with EGTA markedly increased LapA on the cell surface and reduced supernatant LapA, and these effects were partially reversed by the addition of Ca^{2+} (Fig. 2C and D).

We next assessed the potential role of Ca^{2+} in mediating biofilm formation via factors known to impact biofilm formation, such as LapG, LapD, and LapA. As expected, the Δ*lapG* mutant formed a hyperadherent biofilm phenotype in the presence of EGTA alone or in medium with EGTA and $CaCl_2$ (Fig. 2A), as well as in the presence of EGTA and $MgCl_2$ (Fig. 2B). The lack of any impact of these treatments on the phenotype of the Δ*lapG* mutant is reflected in the lack of impact on the level or localization of LapA (Fig. 2C and D).

Interestingly, the Δ*lapD* mutant does not form a biofilm in K10T-1 medium, but the biofilm biomass of the Δ*lapD* strain is significantly increased and approximately three times greater in the presence of EGTA (Fig. 2A), a phenotype reversed by Ca^{2+} (Fig. 2A) but not Mg^{2+} (Fig. 2B). These data suggest that the EGTA-induced hyperadherent biofilm phenotype is independent of LapD.

The hyperadherent biofilm phenotype of the WT and the Δ*lapD* mutant strain treated with EGTA phenocopies that observed in the Δ*lapG* mutant, indicating that Ca^{2+} may mediate biofilm formation via LapG. As a control, we showed that the *lapA* mutant strain does not form a biofilm under any of the conditions tested (Fig. 2A and B), supporting the conclusion that the hyperadherent biofilm phenotypes observed are dependent on the LapA adhesin.

LapG cleavage of LapA requires calcium. One explanation for the similarity in phenotypes between Ca^{2+} chelation and the Δ*lapG* mutant is that the LapG protease requires Ca^{2+} for function. To test this hypothesis, we assessed the ability of LapG to cleave N-Term-LapA in the presence of EGTA and/or Ca^{2+} by

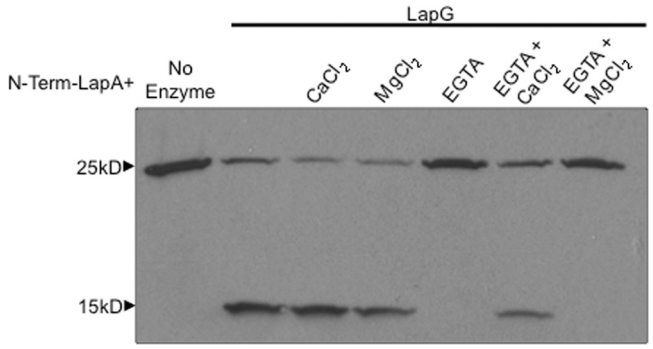

FIG 3 Calcium chelation inhibits LapG protease activity *in vitro*. Shown is a Western blot assay developed with antibodies directed against purified, 6H-tagged N-Term-LapA. N-Term-LapA contains the LapG cleavage site mapped to the N terminus of LapA, as described previously (28). Cleavage of N-term-LapA by LapG results in a shift of the substrate from ~25 kDa to ~15 kDa. The leftmost lane shows the substrate-only control. Under the conditions used here, LapG is able to cleave ~50% of the substrate. The addition to each assay mixture is indicated above the lane. All additions were made to 500 μM.

using an *in vitro* activity assay. Using this assay, we have previously shown that LapG cleaves 10 kDa from the so-called N-Term-LapA construct, which consists of the first 235 amino acids of LapA and contains a 6H epitope tag at its C terminus (28). In this assay, purified LapG and purified N-Term-LapA are coincubated in the presence of EGTA and/or $CaCl_2$ and the cleavage of N-Term-LapA is assessed by SDS-PAGE, followed by Western blotting with an anti-His antibody (28).

In the presence of EGTA, LapG is unable to cleave N-Term-LapA, while in the presence of EGTA and $CaCl_2$, cleavage of N-Term-LapA by LapG is restored. Consistent with a specific role for Ca^{2+}, cleavage is not restored upon the addition of $MgCl_2$ to EGTA-treated assay mixtures (Fig. 3). LapG is able to cleave N-Term-LapA in the presence of $CaCl_2$ or $MgCl_2$ (Fig. 3). These data indicate that LapG-dependent cleavage of N-Term-LapA requires the presence of Ca^{2+}.

Residues D134A and E136A of LapG are required for function. In the accompanying report, Chatterjee and colleagues solved the structure of the LapG homolog from *L. pneumophila* (3). *L. pneumophila* and *P. fluorescens* LapG show 47% and 66% sequence identity and similarity, respectively. Additionally, as with *P. fluorescens* LapG, *L. pneumophila* LapG cleaves N-Term-LapA (3), indicating that the high sequence conservation between these two proteins is reflected in functional conservation of activity. Based on the studies presented here, Chatterjee and colleagues also crystallized *L. pneumophila* LapG in the presence of Ca^{2+} and after EGTA treatment. Ca^{2+} could be modeled at a site adjacent to LapG's catalytic triad only when the protein was crystallized in the presence of this cation. Isothermal titration calorimetry was used to validate and quantify calcium binding (3). Comparison of the Ca^{2+}-bound and Ca^{2+}-free LapG structures indicated that residues D134 and E136 in *P. fluorescens* LapG might be required for Ca^{2+} binding. As shown in the supplemental data of the accompanying report, D134 and E136 flank the catalytic cysteine residues and are 100% conserved in 24 bacterial species (3) and the larger family of DUF920 domain-containing proteins or bacterial transglutaminase-like cysteine proteases (9).

To determine if residues D134 and E136 are required for *P. fluorescens* LapG function, Ala substitutions were constructed and the biofilm phenotype of strains expressing WT LapG, LapG-D134A, or LapG-E136A from a multicopy plasmid was tested. WT LapG and the LapG-D134A and -E136A variants, which were detected via their C-terminal 6H epitope tag, are stably expressed *in vivo* (Fig. 4A, bottom).

Expression of WT LapG from a multicopy plasmid results in no observed biofilm, as expected (28), because overexpression of LapG causes release of LapA into the supernatant from the cell surface (Fig. 4A to C). In contrast, strains expressing the LapG-D134A and LapG-E136A variants resulted in a hyperadherent biofilm phenotype and LapA localization profiles similar to that of the Δ*lapG* mutant strain carrying an empty vector (Fig. 4A to C). These results suggest that residues D134 and E136 are required for LapG function.

Given the apparent lack of function of the LapG-D134A and -E136A mutant proteins *in vivo*, we hypothesized that the Ca^{2+}-binding mutants would be unable to cleave LapA *in vitro*. In these studies, we first prepared a cell extract from the *lapG* mutant carrying a plasmid expressing mini-LapA. Mini-LapA is a smaller constructed variant of LapA consisting of the N and C termini of the protein flanking an internal myc epitope tag (28). This mini-LapA extract served as a substrate to monitor the N-terminal cleavage of LapA. Cell extracts were also prepared from the Δ*lapG* mutant carrying an empty vector, the Δ*lapG* mutant carrying a plasmid overexpressing LapG, or the LapG-D134A or -E136A mutant protein. The mini-LapA- and LapG-containing cell extracts were mixed, and reactions were then analyzed by Western blotting to reveal that mini-LapA cleavage occurs only in the presence of WT LapG and not in the presence of the D134A or E136A LapG variant (Fig. 4D), suggesting that the Ca^{2+}-binding residues are required for mini-LapA cleavage.

We also tested the activity of WT LapG, LapG-D134A, and LapG-E136A by using purified LapG enzymes and substrate. Purified N-Term-LapA was incubated with purified LapG variants. In contrast to WT LapG protein, the LapG-D134A and LapG-E136A variants were unable to cleave N-Term-LapA (Fig. 4E). Taken together, these data support the conclusion that Ca^{2+}-binding residues are required for LapG protease activity.

LapG calcium point mutants cannot interact with LapD. We next assessed if mutation of D134 or E136, in addition to the loss of protease activity, might disrupt the c-di-GMP-dependent interaction between LapG and LapD. Operon constructs of WT LapG and LapD, D134A LapG and WT LapD, or E136A LapG and WT LapD were introduced on a multicopy plasmid into a strain with clean unmarked deletions of the *lapG* and *lapD* genes (Δ*lapG* Δ*lapD*). LapG variants contain an internal HA epitope tag, and LapD contains a 6H epitope tag at its C terminus. Note that in contrast to the data shown in Fig. 4, wherein LapG alone is expressed on a plasmid, here the coexpression of LapD and LapG from a plasmid results in the restoration of a WT phenotype to the Δ*lapG* Δ*lapD* mutant. Cell extracts were prepared to examine the expression of LapG variant and LapD proteins, showing that the proteins are stably expressed (Fig. 5A, bottom).

Because LapG-D134A and -E136A do not complement the Δ*lapG* hyperadherent biofilm phenotype (Fig. 4A), we predicted that LapG-D134A or -E136A introduced on a multicopy plasmid with WT LapD into the Δ*lapG* Δ*lapD* mutant strain would also not be able to complement the Δ*lapG* Δ*lapD* mutant strain's hyperadherent biofilm phenotype. In the Δ*lapG* Δ*lapD* mutant strains, the expression of LapG-D134A or -E136A cannot comple-

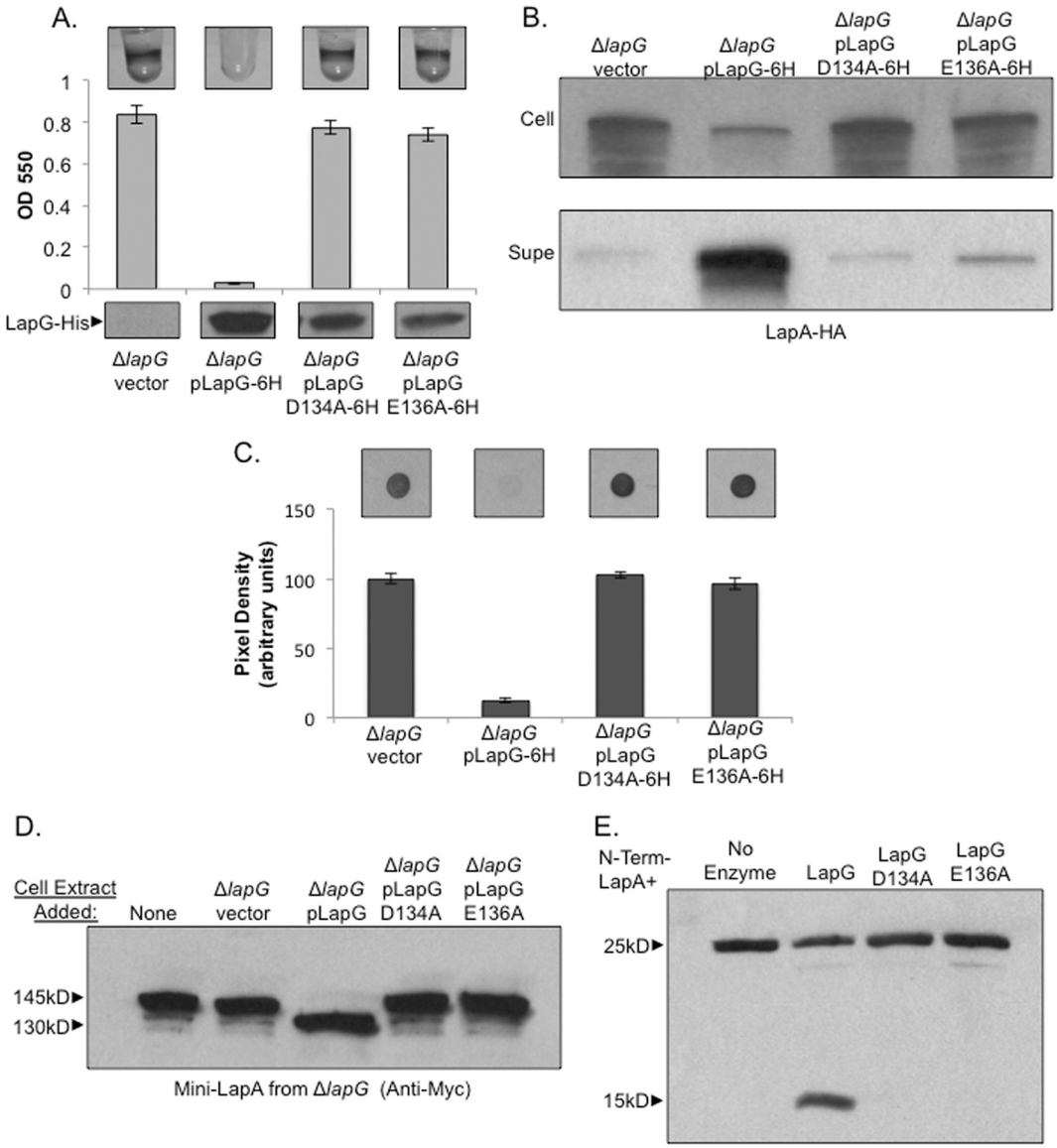

FIG 4 LapG residues D134 and E136 are required for LapG function *in vivo* and *in vitro*. (A) The LapG-D134A and -E136A mutants are stable but nonfunctional *in vivo*. Shown are biofilm assays (top) of the Δ*lapG* mutant strain carrying the vector control or plasmid-expressed WT LapG protein or the LapG-D134A or LapG-E136A mutant protein. The *y* axis shows the optical density at 550 nm (OD 550) of the extracted crystal violet used to determine the bacterial biofilm biomass. Western blotting was used to detect the level of His-tagged WT or mutant protein (bottom). (B) Levels and localization of LapA in whole-cell and supernatant fractions. Shown is a Western blot assay showing the levels of LapA in the whole-cell (Cell) and supernatant (Supe) fractions of the strains indicated. (C) Cell surface levels of LapA. Shown is a representative dot blot assay (top) and quantification of the pixel density of six to eight replicates (bottom) to assess the levels of cell surface LapA of the strains indicated. (D) Mutant LapG proteins cannot cleave mini-LapA in crude extracts. Shown is a Western blot assay detecting mini-LapA with anti-Myc antibodies. Full-length mini-LapA ran at ~145 kDa, while mini-LapA cleaved by LapG migrated at ~130 kDa. Extracts prepared from a Δ*lapG* mutant carrying a plasmid expressing mini-LapA were mixed with the extracts indicated above the blot. (E) Purified LapG mutant proteins are not active *in vitro*. Shown is a LapG activity assay with purified WT or mutant LapG proteins. In this assay, a purified His-tagged portion of the N terminus of LapA was used as the substrate as described in Materials and Methods. The full-length substrate migrated at ~25 kDa, and the cleaved product migrated at ~15 kDa. The LapG protein added to each reaction is indicated above the blot.

ment the hyperadherent biofilm phenotype. In contrast, the Δ*lapG* Δ*lapD* mutant strain overexpressing WT LapG does show a reduction of the hyperadherent biofilm phenotype (Fig. 5A).

Using a coimmunoprecipitation assay, we previously demonstrated that LapD and LapG interact in a c-di-GMP-dependent manner (28). Under the same conditions, a nickel resin was used to pull down LapD-6H and LapG-HA coprecipitation was assessed. WT LapG coprecipitated with WT LapD in the presence of c-di-GMP, with only a weak interaction in the absence of the dinucleotide (Fig. 5B). Neither D134A LapG nor E136A LapG coprecipitated with LapD in the presence or absence of c-di-GMP, suggesting that mutation of the Ca^{2+}-binding residues disrupts the c-di-GMP-dependent interaction between LapD and LapG.

Citrate, a potential environmental source of calcium chelation. The data presented here demonstrate that removal of Ca^{2+} by EGTA chelation and mutation of the LapG Ca^{2+}-binding res-

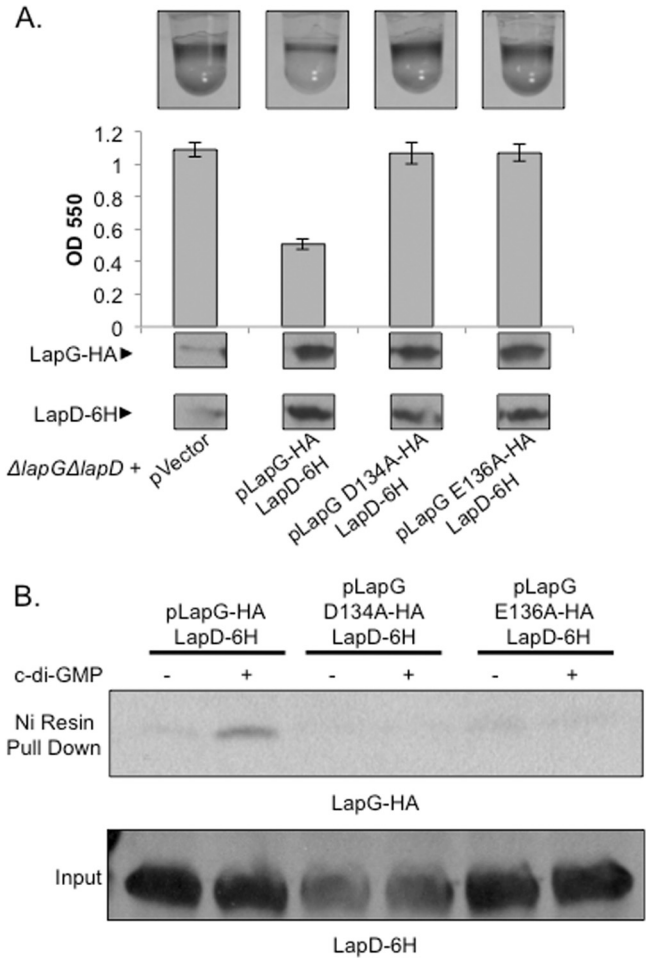

FIG 5 Mutation of LapG residues D134 or E136 to alanine results in loss of interaction with LapD. (A) Biofilm assays with strains used for pulldown studies. Shown are representative biofilm wells (top), quantification of the biofilm assay (middle), and levels of LapG and LapD proteins detected by Western blot assay using anti-HA and anti-6H antibodies (bottom). As outlined in the text, the strains have the expected phenotypes based on the data presented in Fig. 4, and LapG-HA and LapD-6H can be detected at similar levels in the strains expressing WT or mutant LapG. (B) The LapG-D134A and LapG-E136A mutant proteins do not interact with LapD. Shown are Western blot assays from Ni-resin pulldown of LapD-6H using an anti-HA antibody to detect LapG-HA (top) and blots showing the inputs used in these assays (bottom). The strain used to generate the extract used in each lane is indicated above the blot, and the presence or absence of 5 μM c-di-GMP is indicated.

idues induce a hyperadherent biofilm and a nonfunctional LapG protease. These results raise the possibility that absence of Ca^{2+}, potentially due to chelation of this cation, may serve to stabilize a biofilm in the natural environment for this microbe, that is, in soil or on plant roots. We reported previously that citrate, an organic acid and chelating agent (16) stimulated biofilm formation by the *lapD* mutant (11) in a manner analogous to that of EGTA. Furthermore, citrate is found in appreciable levels in the roots and root exudate of plants colonized by *P. fluorescens* (16, 18). Thus, we hypothesized that citrate may serve as a potential environmental source of calcium chelation. To determine whether an environmental and physiologically relevant chelator induced an accumulation of biofilm biomass similarly to EGTA, we assessed biofilm formation in the presence of citrate. A study by Kamilova et al. reported the concentration of citric acid in root exudate of tomato, cucumber, and sweet pepper plants, and high-performance liquid chromatography analysis showed that citric acid concentrations vary depending upon the plant and the growth substrate. Concentrations ranged from 10 to 110 μg/plant (18). Jones reported that the total concentration of organic acids in roots is ~10 to 20 mM (16), while de Weert et al. reported that "studies on tomato exudate have shown that its major components are organic acids (with citric [55.2%], malic [15.3%], and lactic [10%] acids as major components)" (5). Given the variable concentrations of citrate present in the soil and/or in the rhizosphere, we elected to use 0.4% citrate (13.6 mM), the concentration we reported in our previous article (11) and a concentration within the range reported for plant roots (16).

Only a minimal increase in biofilm formation by the WT or the Δ*lapG* mutant is seen in the presence of citrate. Interestingly, for these two strains, the small increase in biofilm formation observed with added citrate is not reduced upon the addition of Ca^{2+}. We do not understand the significance of this finding, but it suggests that for these two strains, the small increase in biofilm formation observed upon citrate addition may be Ca^{2+} independent.

A substantial, significant ($P < 0.05$) increase in biofilm formation is observed in the Δ*lapD* mutant in the presence of added citrate (Fig. 6A), suggesting that chelation by citrate is responsible for increasing biofilm formation. To determine whether the citrate-induced hyperadherent biofilm in the Δ*lapD* mutant is due to Ca^{2+} chelation, biofilm formation was assessed in the presence of citrate and $CaCl_2$. As observed with EGTA and $CaCl_2$ (Fig. 2A), $CaCl_2$ reverses the effects of the citrate-induced hyperadherent biofilm formation in the Δ*lapD* mutant, suggesting that citrate is specifically chelating Ca^{2+}.

Because citrate induces a hyperadherent biofilm in the Δ*lapD* mutant, we hypothesized that citrate, like EGTA, would prevent LapG cleavage of N-Term-LapA *in vitro*. In the presence of citrate, LapG is unable to cleave N-Term-LapA, and furthermore, addition of $CaCl_2$ restored LapG cleavage of N-Term-LapA (Fig. 6B). These data suggest that citrate-mediated Ca^{2+} chelation can effectively inhibit LapG activity *in vitro*.

DISCUSSION

The data presented here and in the accompanying report by Chatterjee and colleagues show that the periplasmic cysteine protease LapG is a Ca^{2+}-containing enzyme and furthermore that binding of this cation is required for LapG activity. This conclusion is supported by chelation studies, genetic analyses, *in vitro* activity assays, and biochemical studies here, as well as analysis of the LapG structure and *in vitro* studies in the accompanying report (3). These studies extend our understanding of this relatively poorly characterized family of DUF920 domain-containing bacterial proteases.

Interestingly, when LapG is unable to bind Ca^{2+}, it also does not interact with LapD in a c-di-GMP-dependent manner. These results suggest that when LapG cannot bind calcium, it also cannot interact with LapD. Presumably, absence of c-di-GMP-dependent LapD regulation of LapG is inconsequential under these circumstances, as the LapG calcium point mutants are nonfunctional. We do not understand why loss of Ca^{2+} impacts the LapD-LapG interaction. It is possible that the site of Ca^{2+} binding and LapD interaction with LapG are proximal, and thus, the observed local alterations in protein structure upon loss of Ca^{2+} could have sec-

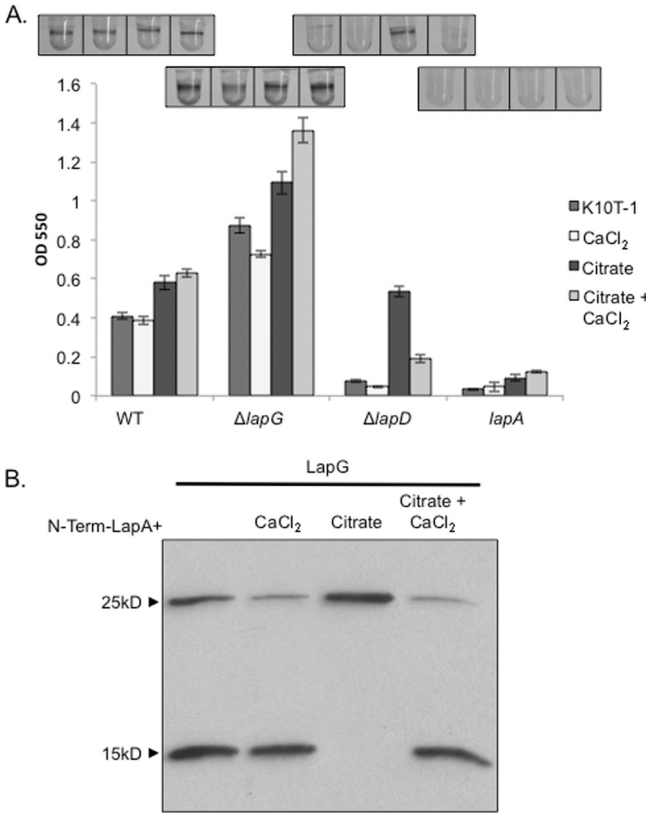

FIG 6 Citrate chelation stimulates biofilm formation. (A) Impact of added citrate on biofilm formation. Shown are biofilm assays of the WT and the Δ*lapG*, Δ*lapD*, and *lapA* mutants grown in K10T-1 medium or in this medium supplemented with $CaCl_2$ (500 μM), citrate (0.4%), or both. The *y* axis shows the optical density at 550 nm (OD 550) of the extracted crystal violet used to determine the bacterial biofilm biomass of the indicated strains. (B) Citrate inhibits LapG activity *in vitro*. Shown is a Western blot developed with antibodies directed against purified, 6H-tagged N-Term-LapA. N-Term-LapA contains the LapG cleavage site mapped to the N terminus of LapA as described previously (28). Cleavage of N-Term-LapA by LapG results in a shift of the substrate from ~25 kDa to ~15 kDa. Under the conditions used here, LapG was able to cleave ~75% of the substrate. The addition to each assay mixture is indicated above the lane. $CaCl_2$ was added to 500 μM, and citrate was added to 0.4%.

ondary effects on LapD binding of LapG. Alternatively, the mutations introduced to disrupt Ca^{2+} binding may have global effects on protein structure resulting in loss of LapD interactions with LapG, although the apparent stability of the LapG mutant variants and the crystallographic analysis of the *L. pneumophila* ortholog argue against gross changes in protein structure. Finally, this Ca^{2+}-dependent interaction with LapD may be an important part of the overall mechanism evolved by *P. fluorescens* to regulate LapG activity and thus biofilm formation. Until we understand more about LapD-LapG interactions, it will not be possible to distinguish among these possibilities.

It is important to note that the periplasmic levels of Ca^{2+} reflect levels in the external environment. Direct measurements of calcium in the periplasm of *E. coli* have been conducted (17). Jones et al. reported that when the external medium contains 0.1 μM free Ca^{2+}, Ca^{2+} is concentrated in the periplasm and the cytoplasm, as the measured concentrations of free Ca^{2+} were 2 to 3 μM and 1 μM, respectively. When the external medium contained 6 μM free Ca^{2+}, the free Ca^{2+} level in the periplasm was 6 μM, while the cytoplasm contained 1 μM free Ca^{2+}. At submicromolar concentrations of free Ca^{2+}, the periplasm and cytoplasm are capable of concentrating free Ca^{2+} (17). The authors state that these results are consistent with the outer membrane being more permeable to Ca^{2+} influx than the inner membrane. Thus, from the studies by Jones et al., it is apparent that Ca^{2+} concentrations fluctuate in the cell in response to the external concentration of Ca^{2+}. Finally, while we do not know the concentration of Ca^{2+} available in our laboratory medium, there is clearly a sufficient amount of this metal present to allow LapG function, as we observe LapG-mediated detachment of biofilms under these laboratory growth conditions.

The finding that citrate, an organic chelator found in niches occupied by *P. fluorescens*, could impact LapG activity via Ca^{2+} chelation suggested the very exciting possibility of an additional environmentally relevant mechanism to regulate biofilm formation by this microbe. It is not clear whether citrate is chelating Ca^{2+} specifically in the soil environment, but in addition to EGTA, this environmentally relevant chelator does exert an effect on biofilm formation and LapG activity, suggesting that the effects observed here for Ca^{2+} chelation are not limited to EGTA. This point is especially intriguing given that the plant root and root exudate environment in which *P. fluorescens* forms biofilms contains many organic acids (5, 16) and that the biofilm matrix is known to be composed of several components, such as extracellular polysaccharide and extracellular DNA, which have substantial Ca^{2+}-chelating activity (7, 25, 36). Thus, exploring the possibility that environmentally relevant organic acids and the biofilm matrix may inhibit cellular functions via the chelation of important metal ions, such as calcium, which contribute to biofilm dispersal is an interesting line for future experimentation.

ACKNOWLEDGMENTS

We thank P. D. Newell for thoughtful discussions and Thomas Hampton for assistance with statistical analysis.

This work was supported by the National Institutes of Health (T32-GM08704 predoctoral fellowship to C.D.B., R01-GM081373 to H.S., and R01 AI097307-01 to H.S. and G.A.O.), a National Science Foundation grant (MCB-9984521 to G.A.O.), and a PEW scholar award in Biomedical Sciences (to H.S.).

REFERENCES

1. **Alonso-GarcíA N, Ingles-Prieto A, Sonnenberg A, de Pereda JM.** 2009. Structure of the Calx-β domain of the integrin β4 subunit: insights into function and cation-independent stability. Acta Crystallogr. D Biol. Crystallogr. **65**:858–871.
2. **Arrizubieta MJ, Toledo-Arana A, Amorena B, Penades JR, Lasa I.** 2004. Calcium inhibits Bap-dependent multicellular behavior in *Staphylococcus aureus*. J. Bacteriol. **186**:7490–7498.
3. **Chatterjee D, Boyd CD, O'Toole GA, Sondermann H.** 2012. Structural characterization of a conserved, calcium-dependent periplasmic protease from *Legionella pneumophila*. J. Bacteriol. **194**:4415–4425.
4. **Dawson RMC, Elliott DC, Elliott WH, Jones KM.** 1986. Data for biochemical research. Clarendon Press, Oxford, United Kingdom.
5. **de Weert S, et al.** 2002. Flagella-driven chemotaxis towards exudate components is an important trait for tomato root colonization by *Pseudomonas fluorescens*. Mol. Plant Microbe Interact. **15**:1173–1180.
6. **Dominguez DC.** 2004. Calcium signalling in bacteria. Mol. Microbiol. **54**:291–297.
7. **Fang Y, et al.** 2007. Multiple steps and critical behaviors of the binding of calcium to alginate. J. Phys. Chem. B. **111**:2456–2462.
8. **Geesey GG, Wigglesworth-Cooksey B, Cooksey KE.** 2000. Influence of calcium and other cations on surface adhesion of bacteria and diatoms: a review. Biofouling **15**:195–205.

9. **Ginalski K, Kinch L, Rychlewski L, Grishin NV.** 2004. BTLCP proteins: a novel family of bacterial transglutaminase-like cysteine proteinases. Trends Biochem. Sci. **29**:392–395.
10. **Haas D, Defago G.** 2005. Biological control of soil-borne pathogens by fluorescent pseudomonads. Nat. Rev. Microbiol. **3**:307–319.
11. **Hinsa SM, O'Toole GA.** 2006. Biofilm formation by *Pseudomonas fluorescens* WCS365: a role for LapD. Microbiology **152**:1375–1383.
12. **Hinsa SM, Espinosa-Urgel M, Ramos JL, O'Toole GA.** 2003. Transition from reversible to irreversible attachment during biofilm formation by *Pseudomonas fluorescens* WCS365 requires an ABC transporter and a large secreted protein. Mol. Microbiol. **49**:905–918.
13. **Holland IB, Jones HE, Campbell AK, Jacq A.** 1999. An assessment of the role of intracellular free Ca^{2+} in *E. coli*. Biochimie **81**:901–907.
14. **Jackson DW, Simecka JW, Romeo T.** 2002. Catabolite repression of *Escherichia coli* biofilm formation. J. Bacteriol. **184**:3406–3410.
15. **Jackson DW, et al.** 2002. Biofilm formation and dispersal under the influence of the global regulator CsrA of *Escherichia coli*. J. Bacteriol. **184**: 290–301.
16. **Jones DL.** 1998. Organic acids in the rhizosphere—a critical review. Plant Soil **205**:25–44.
17. **Jones HE, Holland IB, Campbell AK.** 2002. Direct measurement of free Ca^{2+} shows different regulation of Ca^{2+} between the periplasm and the cytosol of *Escherichia coli*. Cell Calcium **32**:183–192.
18. **Kamilova F, et al.** 2006. Organic acids, sugars, and L-tryptophane in exudates of vegetables growing on stonewool and their effects on activities of rhizosphere bacteria. Mol. Plant Microbe Interact. **19**:250–256.
19. **Lugtenberg BJ, Kravchenko LV, Simons M.** 1999. Tomato seed and root exudate sugars: composition, utilization by *Pseudomonas* biocontrol strains and role in rhizosphere colonization. Environ. Microbiol. **1**:439–446.
20. **MacEachran DP, Stanton BA, O'Toole GA.** 2008. Cif is negatively regulated by the TetR family repressor CifR. Infect. Immun. **76**:3197–3206.
21. **Matsuoka S, et al.** 1995. Regulation of the cardiac Na^{+}-Ca^{2+} exchanger by Ca^{2+}. Mutational analysis of the Ca^{2+}-binding domain. J. Gen. Physiol. **105**:403–420.
22. **Michiels J, Xi C, Verhaert J, Vanderleyden J.** 2002. The functions of Ca^{2+} in bacteria: a role for EF-hand proteins? Trends Microbiol. **10**:87–93.
23. **Monds RD, Newell PD, Gross RH, O'Toole GA.** 2007. Phosphate-dependent modulation of c-di-GMP levels regulates *Pseudomonas fluorescens* Pf0-1 biofilm formation by controlling secretion of the adhesin LapA. Mol. Microbiol. **63**:656–679.
24. **Monds RD, Newell PD, Schwartzman JA, O'Toole GA.** 2006. Conservation of the Pho regulon in *Pseudomonas fluorescens* Pf0-1. Appl. Environ. Microbiol. **72**:1910–1924.
25. **Mulcahy H, Charron-Mazenod L, Lewenza S.** 2008. Extracellular DNA chelates cations and induces antibiotic resistance in *Pseudomonas aeruginosa* biofilms. PLoS Pathog. **4**:e1000213. doi:10.1371/journal.ppat.1000213.
26. **Navarro MV, et al.** 2011. Structural basis for c-di-GMP-mediated inside-out signaling controlling periplasmic proteolysis. PLoS Biol. **9**:e1000588. doi:10.1371/journal.pbio.1000588.
27. **Newell PD, Monds RD, O'Toole GA.** 2009. LapD is a bis-(3′,5′)-cyclic dimeric GMP-binding protein that regulates surface attachment by *Pseudomonas fluorescens* Pf0-1. Proc. Natl. Acad. Sci. U. S. A. **106**:3461–3466.
28. **Newell PD, Boyd CD, Sondermann H, O'Toole GA.** 2011. A c-di-GMP effector system controls cell adhesion by inside-out signaling and surface protein cleavage. PLoS Biol. **9**:e1000587. doi:10.1371/journal.pbio.1000587.
29. **Newell PD, Yoshioka S, Hvorecny KL, Monds RD, O'Toole GA.** 2011. Systematic analysis of diguanylate cyclases that promote biofilm formation by *Pseudomonas fluorescens* Pf0-1. J. Bacteriol. **193**:4685–4698.
30. **Norris V, et al.** 1991. Calcium in bacteria: a solution to which problem? Mol. Microbiol. **5**:775–778.
31. **Norris V, et al.** 1996. Calcium signalling in bacteria. J. Bacteriol. **178**: 3677–3682.
32. **O'Toole GA, Kolter R.** 1998. Initiation of biofilm formation in *Pseudomonas fluorescens* WCS365 proceeds via multiple, convergent signalling pathways: a genetic analysis. Mol. Microbiol. **28**:449–461.
33. **O'Toole GA, Gibbs KA, Hager PW, Phibbs PV, Jr, Kolter R.** 2000. The global carbon metabolism regulator Crc is a component of a signal transduction pathway required for biofilm development by *Pseudomonas aeruginosa*. J. Bacteriol. **182**:425–431.
34. **Prigent-Combaret C, Vidal O, Dorel C, Lejeune P.** 1999. Abiotic surface sensing and biofilm-dependent regulation of gene expression in *Escherichia coli*. J. Bacteriol. **181**:5993–6002.
35. **Prigent-Combaret C, et al.** 2001. Complex regulatory network controls initial adhesion and biofilm formation in *Escherichia coli* via regulation of the *csgD* gene. J. Bacteriol. **183**:7213–7223.
36. **Sarkisova S, Patrauchan MA, Berglund D, Nivens DE, Franklin MJ.** 2005. Calcium-induced virulence factors associated with the extracellular matrix of mucoid *Pseudomonas aeruginosa* biofilms. J. Bacteriol. **187**: 4327–4337.
37. **Sauer K, et al.** 2004. Characterization of nutrient-induced dispersion in *Pseudomonas aeruginosa* PAO1 biofilm. J. Bacteriol. **186**:7312–7326.
38. **Schwarz EM, Benzer S.** 1997. Calx, a Na-Ca exchanger gene of *Drosophila melanogaster*. Proc. Natl. Acad. Sci. U. S. A. **94**:10249–10254.
39. **Shanks RM, Caiazza NC, Hinsa SM, Toutain CM, O'Toole GA.** 2006. *Saccharomyces cerevisiae*-based molecular tool kit for manipulation of genes from Gram-negative bacteria. Appl. Environ. Microbiol. **72**:5027–5036.
40. **Singh PK, Parsek MR, Greenberg EP, Welsh MJ.** 2002. A component of innate immunity prevents bacterial biofilm development. Nature **417**: 552–555.
41. **Smith RJ.** 1995. Calcium and bacteria. Adv. Microb. Physiol. **37**:83–133.
42. **Theunissen S, et al.** 2010. The 285 kDa Bap/RTX hybrid cell surface protein (SO4317) of *Shewanella oneidensis* MR-1 is a key mediator of biofilm formation. Res. Microbiol. **161**:144–152.
43. **Thormann KM, et al.** 2006. Control of formation and cellular detachment from *Shewanella oneidensis* MR-1 biofilms by cyclic di-GMP. J. Bacteriol. **188**:2681–2691.
44. **Tsien RY.** 1980. New calcium indicators and buffers with high selectivity against magnesium and protons: design, synthesis, and properties of prototype structures. Biochemistry **19**:2396–2404.